Joint EPRI – 123HiMAT International Conference on
Advances in High Temperature Materials
October 21–24, 2019, Nagasaki, Japan
J. Shingledecker, M. Takeyama, editors
https://doi.org/10.31339/asm.cp.am-epri-2019p0315

THE DEVELOPMENT OF NONDESTRUCTIVE EVALUATION COUPONS IN FULL GRADE 91 CROSS-WELDS WITH VARIOUS LEVELS OF CREEP DAMAGE

Alex Bridges, John Siefert, Jay Richardson
Electric Power Research Institute, 1300 WT Harris Blvd., Charlotte, NC 28262

ABSTRACT

The global electric power production is largely dependent on the operation of fossil-fired generation units. Many coal-fired units are exceeding 300,000 hours, which is beyond the expected design life. This has caused a continuous need to inspect steam touched components operating at high temperature and pressure. State-of-the-art coal and combined cycle gas units are specifying ever-greater amounts of the Creep Strength Enhanced Ferritic (CSEF) steels such as Grade 91 or Grade 92. The martensitic 9%Cr CSEF steels were developed to provide greater strength than traditional low alloy power plant steels, such as Grades 11, 12 and 22. The enhanced strength allows for a reduction in overall wall thickness in new or replacement components. Extensive research in both service failures and laboratory testing has shown that time-dependent creep damage can develop differently in Grade 91 steel when compared to low alloy steels. Furthermore, the creep strength in Grade 91 can vary by more than a factor of 10 between different heats. This wide variation of creep strength has led to extensive research in understanding the damage mechanisms and progression of damage in this steel.

In this study, large cross weld samples were fabricated from thick wall piping in Grade 91 steel using two different heats of material. One weld was fabricated in a 'damage tolerant' heat and another weld was fabricated in a 'damage intolerant' heat of material. The samples were subjected to a post-weld heat treatment (PWHT) at a temperature of 745°C (1375°F) for 1.50 hours. Hardness maps were collected on the cross-welds in the as-welded and PWHT condition for both weldments. Cross-weld creep test conditions were selected to develop accelerated damage representative of in-service behavior. The test samples were interrupted at multiple stages and nondestructively evaluated (NDE) with advanced phased-array ultrasonic techniques. Samples were developed to variable levels of damage (50% to 100% life fraction) in both weldments. Metallographic sections were extracted at specific locations to validate the NDE findings using light emitting diode, laser and scanning electron microscopy. This research is being used to help validate the level of damage that can be reliably detected using conventional and advanced NDE techniques.

INTRODUCTION

High energy piping (HEP) used in both coal-fired and natural gas power plants utilize both low alloy steels and Creep Strength Enhanced Ferritic (CSEF) steels. Common low alloy steels in HEP systems consist of Grade 11 or Grade 22. HEP systems which specify CSEF steels utilize Grade 91 or Grade 92. Ultimately, the decision to select a specific material is driven by the expected in service stress and design temperature such that the migration to CSEF steels is driven by a need to take advantage of the materials' higher strength. HEP systems are subdivided into additional types; the systems which experience time-dependent damage are those classified as the main steam, hot reheat or turbine piping. The main steam piping carries large volumes of steam from the boiler (starting from the superheat outlet) to the high-pressure (HP) turbine. The exhaust steam is sent back to the boiler and reheated before being carried through the hot reheat piping

system, which carries steam to the intermediate pressure (IP) turbine. Creep is a slow time-dependent plastic deformation process that occurs when materials are subjected to both high temperatures and stresses. This time-dependent deformation process can cause creep cavitation damage to occur at locations of high stress. Areas of high stress are typically found at bends, elbows, seam-welds, and transitions where girth welds are located. Additionally, the material properties can have a very profound effect on the initiation and evolution of creep damage in susceptible locations in the system. Extensive research has been conducted to show the effects of piping geometries, weld geometries, and material properties on the effect of creep cavitation and damage progression [1-7].

The consequence of failure in HEP systems is typically very high such that a leak or break can occur in areas of high human traffic, pose complications to collateral damage, or impose long lead times for local component replacement or repair operations to mitigate damage. Thus, non-destructive examination methods have traditionally been a cornerstone of the life management strategy of HEP systems to assess component or system health. Typical methods are segmented into surface or volumetric types including: magnetic particle, liquid penetrant, radiography and ultrasonic testing (and its variants).

The focus of this paper will be on the development of a well-characterized set of damage in carefully controlled cross-weld creep specimens in a feature type sample geometry using two different heats of Grade 91 steel. The gauge section of the feature cross-weld creep samples contains the entirety of the weld including through-weld-thickness of 38 mm (1.50 in.) or 50 mm (2.00 in.). The two heats of Grade 91 steel are of specific interest as they exhibit very different cross-weld creep responses and represent a range in damage manifestation that NDE can be expected to identify in the field. The two heats thus represent a 'damage tolerant' material and the second a 'damage intolerant' material. The importance between the two materials and their implications in NDE phased array ultrasonic inspection techniques is discussed.

EXPERIMENTAL DETAILS

Damage Tolerant and Damage Intolerant Material

The damage tolerant heat of Grade 91 was fabricated to ASTM A335 specifications [8]. The spool piece was approximately 914 mm (36 in.) in length with an outer diameter (OD) of 457 mm (18 in.) and a wall thickness of 39.6 mm (1.56 in.) The P91 piping spool was saw cut into halves along the girth and weld prep angles were machined. The weld profile used a 37.5° angle from the inner diameter (ID) to mid-wall and a transition to a 10° angle from mid-wall to the OD. The piping spool geometry and weld profile is shown in Fig 1.

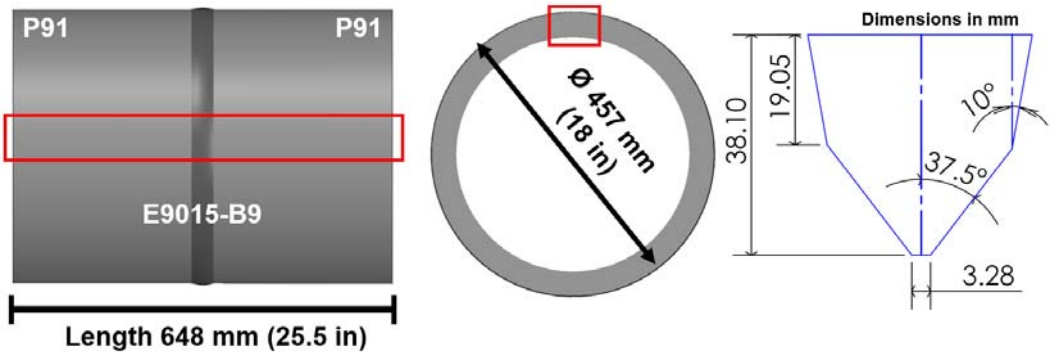

Figure 1: Fabrication and weld profile geometry for damage tolerant heat of Grade 91

The damage intolerant material was selected from an ex-service high temperature secondary superheat outlet header removed from service after extensive damage in the tube to header connections in 89,000 hours. The identified damage in this header is previously detailed in [9]. The section was 914 mm (36 in.) in length with a 457 mm (18 in.) OD and a wall thickness of 53.3 mm (2.1 in.). The weld profile was comparable the damage tolerant material, with a 37.5° angle from the ID to 1/3rd the wall and transitioning to a 10° angle to the OD. Due to dimensional limitations, extension pieces where welded on each end of the material before sample extraction. This allowed the sample size to be of sufficient length for creep testing (shown in Fig 2).

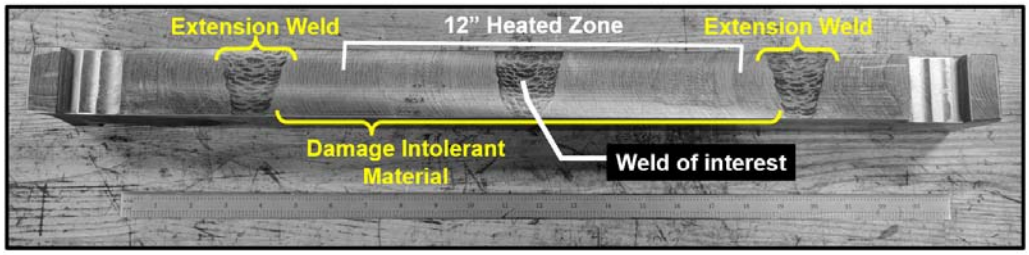

Figure 2: Machined sample with extension welds in damage intolerant material

The welding parameters were kept constant for both heats of material. A large positioner was used to automatically rotate the piping spool in the damage tolerant heat. The damage intolerant was welded using a backing ring in a fixed position. The following details the welding process utilized for both weldments:

1. Root gap was specified to 3.2 mm (0.125 in.)
2. The minimum preheat temperature was 150°C (300°F)
3. The maximum interpass temperature was 315°C (600°F)
4. The sections were maintained at the preheat temperature until completion of the weld
5. The root pass and hot pass were performed using the gas tungsten arc welding (GTAW) process
6. The shielded metal arc welding (SMAW) process was used for the balance of the fill layers including a 3.2 mm (0.125 in.) diameter E9015-B9 electrode for the first layers; and a 4.0 mm (0.157 in.) electrode for the remaining layers.
7. Each layer was grounded lightly after each layer to remove the potential introduction of slag inclusions into the body of the weld volume. Gross introduction of such flaws would have complicated the inspection process and were purposely avoided for this set of welds.

The chemical composition in the damage tolerant and damage intolerant material was measured and compared to the chemical composition requirements by ASME Section IIA for P91 SA 335 material. Additionally, comparisons are shown to the ASME Code Case 2864 (now included for common product forms in ASTM/ASME A/SA-specs as 'Type II'), which sets stricter chemistry requirements for Grade 91 (9Cr-1Mo-V) material. The implications of chemical composition on the creep behavior and detectability of damage using non-destructive phased array techniques in Grade 91 cross-welds is deliberated in the discussion section. Although the damage intolerant heat contains elevated amounts of elements like S or Al, at the time of fabrication and installation of the material in the plant the Grade 91 steel was code-compliant.

Table 1: Chemical composition for damage tolerant and damage intolerant heats compared to requirements in ASME SA335 (prior to 2005) and ASME CC2864 (current to 2018)

Material	**C**	**Mn**	**P**	**S**	**Si**	**Cr**	**Mo**
Damage Tolerant	0.117	0.49	0.011	0.0017	0.365	8.609	0.92
Damage Intolerant	0.080	0.41	0.012	0.009	0.14	8.88	0.93
ASME SA335	0.08-0.12	0.30-0.60	0.020	0.010	0.20-0.50	8.0-9.5	0.85-1.05
ASME CC 2864	0.08-0.12	0.30-0.50	0.020	0.005	0.20-0.40	8.0-9.5	0.85-1.05
Material	**W**	**Ni**	**V**	**Nb**	**N**	**Cu**	**Al**
Damage Tolerant	<0.002	0.12	0.236	0.067	0.0440	0.107	0.009
Damage Intolerant	<0.002	0.0447	0.21	0.061	0.0447	0.18	0.034
ASME SA335	-	0.40	0.18-0.25	0.06-0.10	0.030-0.070	-	0.040
ASME CC 2864	0.05	0.20	0.18-0.25	0.06-0.10	0.035-0.070	0.10	0.020
Material	**B**	**Ti**	**Zr**	**As**	**Sn**	**Sb**	**N/Al (min)**
Damage Tolerant	0.0004	0.002	<0.002	0.003	0.007	0.0013	4.89
Damage Intolerant	<0.001	<0.001	<0.002	0.0136	0.0083	0.0019	1.31
ASME SA335	-	0.01	0.01	-	-	-	-
ASME CC 2864	0.001	0.01	0.01	0.010	0.010	0.003	4.0

Experimental Procedures for Testing

Macro sections from each heat of material were cut and polished for hardness evaluation. Sections from each heat were also post-weld heat treated (PWHT) at 750°C (1375°F) for 1.50 hours. The as-welded and PWHT macro sections were polished to a 1 µm finish using standard metallographic techniques. An automated Vicker's hardness machine (LECO AMH 243) was used to assess a 25 x 25 mm (1 x 1 in.) location in the weldment containing portions of the major constituents (weld, HAZ and base metal). A testing load of 500 grams and an indent spacing of 250 µm was utilized to produce a hardness map containing 10,000 total indents.

Creep samples were extracted from the fabricated weldment and given a PWHT of 750°C (1375°F) for 1.50 hours. The overall sample size for the damage tolerant material was 648 mm (25.5 inch) in length, 50.8 mm (2.00 in.) across the width and 38.1 mm (1.50 in.) in thickness (weld depth). The overall sample size for the damage intolerant material was 648 mm (25.5 inch) in length, 63.5 mm (2.50 in.) across the width and 50.8 mm (2.00 in.) in thickness (weld depth). A 222 kN (50,000 lb-f) dead-weight creep frame was used. The measured temperature variation across the 100 mm (4 in.) gauge section was kept within ±2°C (±3°F).

Two different approaches were taken for non-destructive examination of the large creep samples. The first consisted of routine interruptions throughout the life of each test. This involved detailed non-destructive examinations using phased-array ultrasonic testing (PAUT) methods to evaluate the extent of damage, and to make comparisons of the data to previous interruptions. The second approach involved a single interruption at a known time and/or strain fractions based on previous sample test results. The examination of creep test samples was performed with a 10 MHz transducer with 64 elements and mounted on a 36° shear mode rexolite wedge. A half-path focal law was created to provide beam steering and focusing along the weld HAZ. System sensitivity calibration was performed on a calibration block manufactured from extra material removed from the same Grade 91 test material. The block contained 1.25 mm (0.05 in.) side drilled holes (SDH), aligned at a separation of 0.63 mm (0.25 in.) center to center that simulated the specimen weld profile. The probe was positioned on the calibration block at the first setback distance determined during examination coverage planning. The response from the SDH located at 4/5t is maximized to determine the reference sensitivity setting. An additional 10 Db of system gain is added during scanning.

Metallographic sections were also taken from each test to draw comparisons to the findings from PAUT. These sections were removed using electric discharge machining (EDM) methods to

minimize the amount of removed material to allow for further NDE PAUT scans. The polished macro-sections were evaluated using a light-emitting-diode wide-area scanner (Keyence VR-3200) for macro imaging. Detailed damage evaluations were conducted using information gathered on a confocal laser microscope (Keyence VK-X105) using a 20X lens (~400X magnification). Each individual image had a 700 µm by 525 µm field of view with a pixel resolution of 1024 x 768 and approximately 18.5% overlap to allow for sufficient image stitching. The grid size was 10 by 27 (270 images), giving a total pixel resolution of 8666 x 17331 (image size of 5907 µm by 11813 µm). The fusion boundary was traced to allow for calculation of individual creep voids as a function of the distance from the weld fusion boundary.

RESULTS

Hardness Testing

The average hardness in the weld metal (WM) was approximately 350 to 450 HV 0.5 for both weldments. After post-weld heat treated at 750°C (1375°F) for 1.50 hours, the WM hardness reduced to approximately 240 HV 0.5 and 260 HV 0.5 in the damage tolerant and damage intolerant material, respectively. Detailed hardness maps for each of condition in both heats of material is shown in Fig 3.

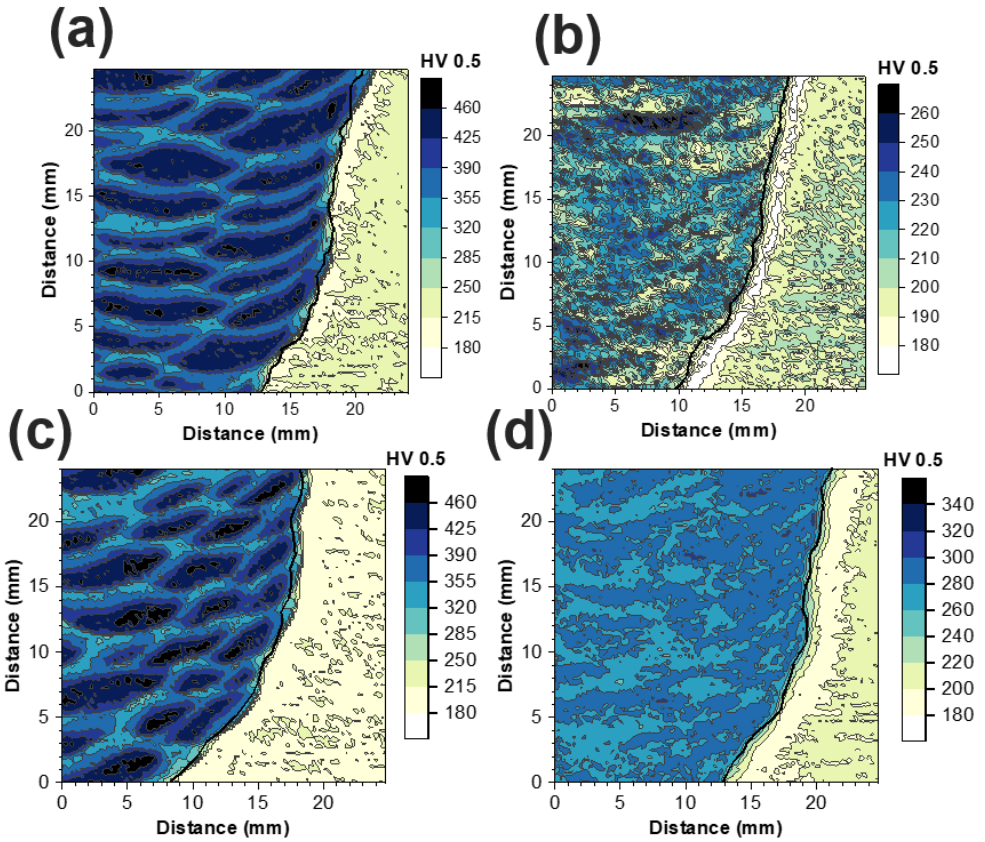

Figure 3: (a) hardness map for damage tolerant material in the as welded condition. (b) hardness map for damage tolerant material in the post-weld heat treated condition. (c) hardness map for damage intolerant material in the as welded condition. (d) hardness map for damage intolerant material in the post-weld heat treated condition.

Creep Testing

Creep testing was conducted on samples from each heat of material in large 222 kN (50,000 lb-f) dead-weight creep frames at a constant load and temperature. The testing matrix for each test is shown in Table 2. All tests were interrupted before rupture and selected tests had routine interruptions throughout the life of the sample. Testing conditions were selected to produce relevant damage accumulation that would be comparable to that found in service components. These conditions were informed by a large dataset assembled by EPRI including more than a decade of internal testing and external collaboration to inform a relevant set of test outcomes [10].

Table 2: Testing matrix for damage tolerant and damage intolerant full cross-weld creep tests

ID*	NDE Interruptions	Temperature		Stress		Stopped Time
	% life	°C	°F	MPa	ksi	(estimated life)
DT-1	49%, 59%, 60%, 68%, 80%, 89%, 92%, 94%	625	1157	80	11.6	(~94%)
DT-2	99%	650	1202	80	11.6	(~99%)
DT-3	43%, 81%	650	1202	80	11.6	(~81%)
DINT-4	24%, 43%, 58%, 64%, 70%, 83%, 90%, 95%	625	1202	60	8.7	(~95%)
DT-5	54%	650	1157	80	11.6	(~54%)
DINT-6	99%	625	1202	60	8.7	(~99%)

*DT = damage tolerant; DINT = damage intolerant

Full cross-weld creep samples in damage tolerant material included one test at a temperature of 625°C (1157°F) and three additional tests at a temperature of 650°C (1202°F). All tests in the damage tolerant material were subjected to the same uniaxial testing stress of 80 MPa (11.6 ksi).

Samples in the damage intolerant material had two tests that were conducted at the same temperature of 625°C (1157°F) and uniaxial stress of 60 MPa (8.7 ksi). The lower temperature and stress was selected because the base material exhibited lower bound creep behavior and creep ductility. Previous EPRI studies have conclusively shown that the preferred test condition to generate extensive damage in Grade 91 steel cross-weld tests, regardless of parent metal condition, is 625°C (1157°F) and 60 MPa (8.7 ksi). Calculations of life percentages were based on time/strain curves gathered from each creep test.

Non-destructive Examination and Metallography

At least one creep sample from both heats of material was selected for routine interruptions throughout the life of the cross-weld. After each interruption, the sample was evaluated using PAUT in a laboratory setting under well controlled conditions. The damage tolerant (ID: DT-1) sample was interrupted a total of 8 times and evaluated using PAUT under the same settings. Figure 6 shows the progression of scans at each interrupted stage from 0.49 to 0.94 life fractions. NDE PAUT techniques successfully identified a potential indication at 80% life fraction and subsequent scans validated the indication showing growth of a linear defect and/or alignment of multiple linear defects at a specific location. All scans shown in Fig. 4 were taken at the same location across the width of the sample (~ 15 mm from a free surface). A summary of NDE findings are shown in Table 3.

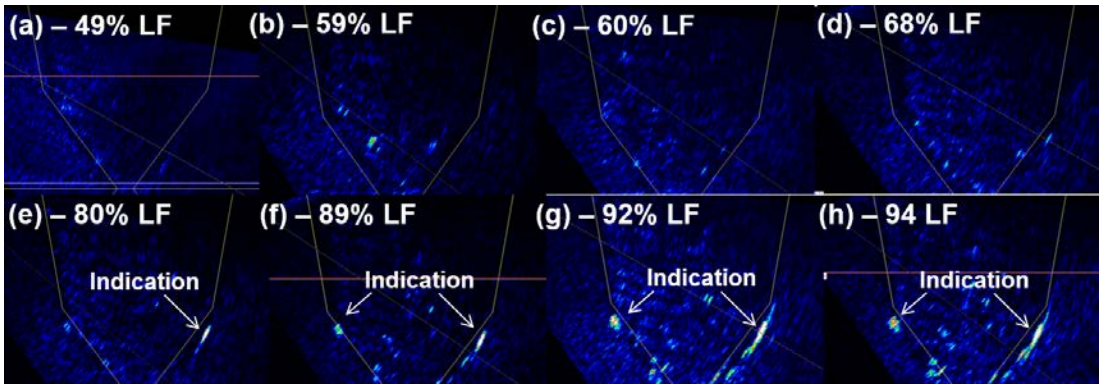

Figure 4: Non-destructive examination scans after various interruptions for damage tolerant sample DT-1 (final interruption at ~ 94% life). Initial indications noted at 80% life fraction.

Table 3: Summary of NDE examination findings in damage tolerant sample DT-1

Interruption	Estimated Life Fraction	Non-Destructive Examination Finding
1	~ 49%	No indications
2	~ 59%	No indications
3	~ 60%	No indications
4	~ 68%	Potential indications; potential signal consistent with early stage creep damage
5	~ 80%	Indications; signal consistent with previous stages, formation of creep cavities along upstream HAZ
6	~ 89%	Indications; signal consistent with previous stages, formation of creep cavities along upstream HAZ
7	~ 92%	Clear increase in signal/indication from previous interruption
8	~ 94%	Similar signal (slight increase) to 7th interruption

A metallographic cross section was taken from the routinely interrupted (DT-2) damage tolerant sample. Creep cavitation was noted along the entire HAZ on both sides of the weld. Localized micro-cracking was shown mid-wall near the weld bevel transition. These locations match with the indications found from NDE PAUT. Figure 5 shows the macro damage that accumulated in the HAZ of the cross-weld. The micro-cracks were found to range in size from 0.2 to 0.5 mm, but the total alignment of microcracks was approximately 3 mm in length. The final estimated life fraction in this sample was approximately 94%.

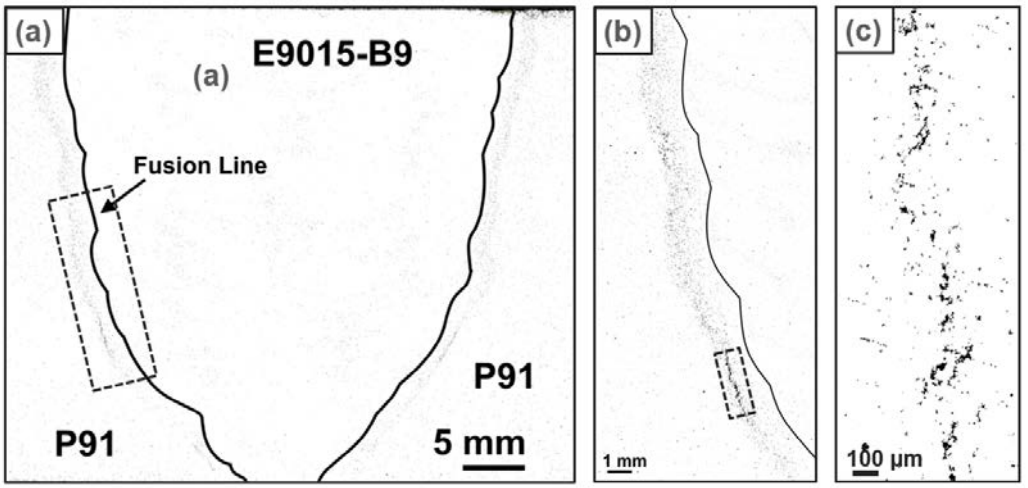

Figure 5: Macro images of removed and polished metallographic sections from damage tolerant sample DT-1 (~94%). (a) macro image of damage of the full cross-section weld depth. (b) macro image of the left side HAZ. (c) macro image of micro-cracking in left HAZ.

Damage tolerant sample DT-2 was interrupted once, right before rupture. It is estimated that this sample was near the very end of life due to the very sharp uptake in strain rate right before interruption. NDE PAUT succesfully indiated the large macro crack, as well as the micro-cracking on the opposite side. The large macro crack initated mid-wall near the weld bevel transition and grew in both directions. It is estimated that this sample was ~99% life fraction.

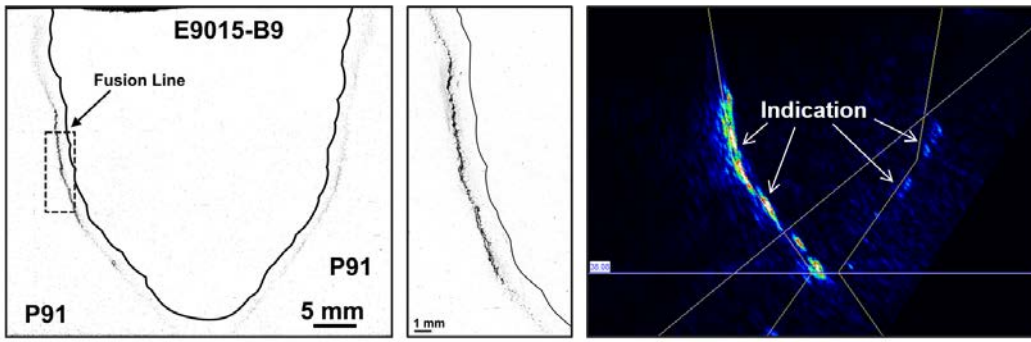

Figure 6: Macro images of removed and polished metallographic section from damage tolerant sample DT-2 (~99%) compared to NDE PAUT scan data.

The damage intolerant heat (DINT-4) was interrupted a total of 8 times throughout the life of the cross-weld. NDE PAUT scans at each interruption is shown in Fig 7. Although the estimated life fraction was ~95%, there were no signs or indications of damage at any stage (via NDE). Metallographic macro sections showed very dense populations of creep cavitation in the heat affected zone on both sides of the cross-weld. The large densities of damage did not result in a linear crack with sufficient length for detection using PAUT. This result suggests that conventional PAUT is unable to characterize and/or detect high densities of creep damage unless a linear defect/crack has propagated to a critical length. This critical length has often been specified to be on the order of 1 to 3 mm, such as in [11].

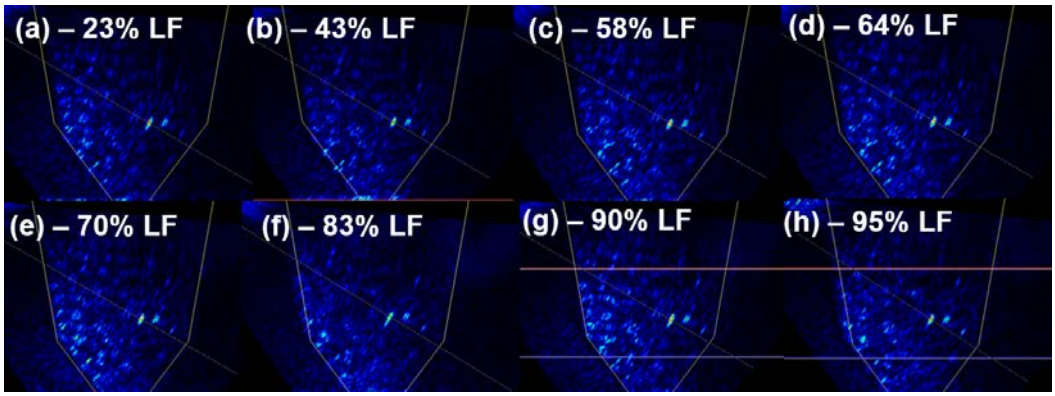

Figure 7: Non-destructive examination scans after various interruptions for damage intolerant sample DINT-4 (final interruption at ~ 95% life). No indications noted at any stage.

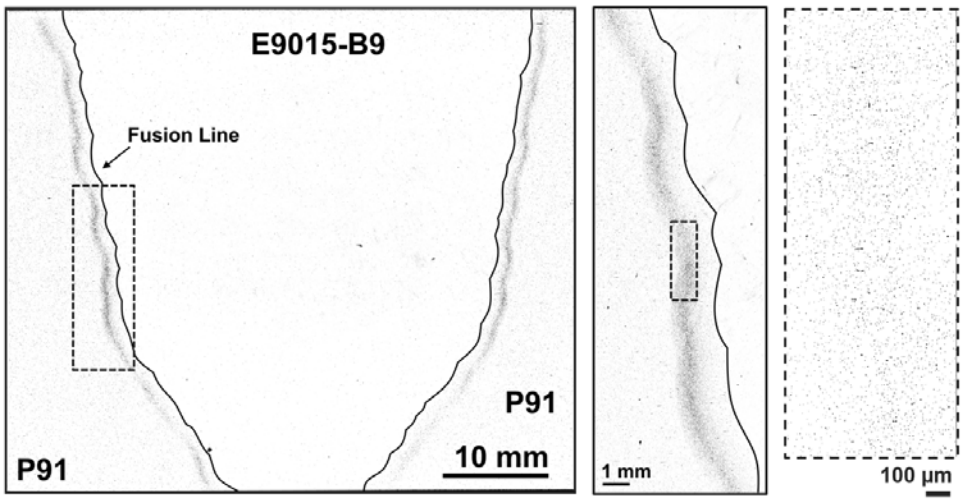

Figure 8: Macro images of removed and polished metallographic section from damage intolerant sample DINT-4 (~95%). Zoomed images so the very high densities of creep voids in the left HAZ.

The damage intolerant heat (DINT-6) was interrupted after 2,648 hours due to a sharp uptake in strain rate (comparable to that in DT-2). NDE PAUT successfully found the large >90% through wall macro crack on the right side of the cross weld. NDE also showed some low signal indications on the opposite side of the cross-weld. The HAZ region opposite the macro-cracked side of the weld likely had some micro-cracking in various locations throughout the weld. The metallographic sample showed very high accumulations of creep voids in this area. Fig. 9 shows the macro damage from metallographic sectioning and corresponding NDE PAUT indications.

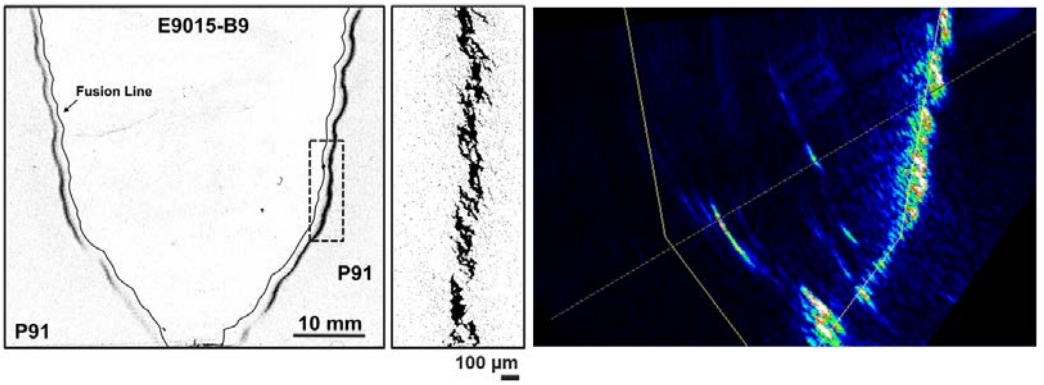

Figure 9: Macro images of removed and polished metallographic section from damage intolerant sample DINT-6 (~99%) compared to NDE PAUT scan data.

DISCUSSION

Damage Manifestation and Creep Void Density

The two different heats of material showed stark differences in the manifestation and evolution of damage. This is largely due to the variation in chemical composition of the two different materials. The damage intolerant material showed higher amounts of trace elements, such as sulfur, aluminum, tin, antimony and copper. Research has shown that these elements can reduce creep strength and creep ductility if presence in Grade 91 steel [7]. Grade 91 steel is a tempered martensitic steel that is strengthened by high densities of dislocations and elements that provide solid solution strengthening. Additionally, it is strengthened by precipitation of vanadium (V) and niobium (Nb) carbon nitrides (MX type) at defect sites and lath boundaries. Alloys that have large amounts of aluminum (damage intolerant heat) are susceptible to the formation of aluminum nitrides (AlN). This is because aluminum is a strong nitride former and AlN's have the tendency to form before vanadium and/or niobium carbon nitrides. Table 4 show deleterious elements that cause both strength and ductility reductions in the damage intolerant heat.

Table 4: Effects of tramp elements on the creep behavior in Grade 91 steel

Element	Effect on Creep Properties
Tin (Sn)	Has shown to reduced creep strength (no effect at temperatures <550 °C) and shown to accumulate at subgrain boundaries
Antimony (Sb) Arsenic (As)	Has the tendency to segregate to grain boundaries and other defects at melting and other high temperature processes; causing creep embrittlement
Copper (Cu)	Has shown to reduce creep ductility; rupture life independent of Cu wt. % and recommended to be below 0.10 wt. %
Sulfur (S)	Experimental studies have shown relationship between S level and time to failure, additional, increased S may result in larger quantities of MnS inclusions
Aluminum (Al)	In heats with low N:Al ratios, N is consumed by formation of AlN and prevents formation of beneficial MX carbonitrides

Creep strength in the damage intolerant heat is reduced by more than an order of magnitude (10-15 times), thus it was relevant to reduce the testing temperature and stress to produce similar rupture times in this heat of material. The tests that were ran to > ~95% life was plotted against literature cross-weld creep data for Grade 91 in Fig 10.

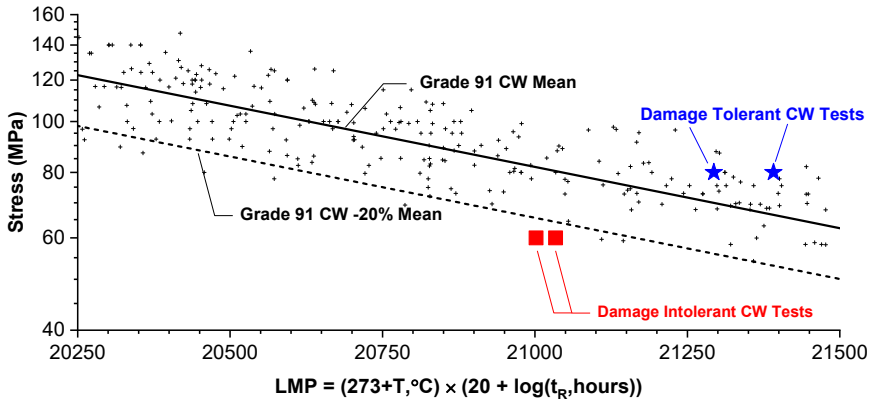

Figure 10: Stress vs. Larson-Miller parameter of damage tolerant and damage intolerant tests (DT-1, DT-2, DINT-4 and DINT-6) compared to literature Grade 91 CW data.

Two macro samples were chosen for detailed analysis of the damage accumulation using a systematic assessment of the creep void density through the HAZ. The procedure utilized is consistent with the detailed process in [12]. Damage tolerant sample DT-1 (~95% life) and damage intolerant sample DINT-4 (~95%) were chosen for a direct comparison of creep damage at a similar life fraction. The combined void maps and distribution of damage for both DT-1 and DINT-4 is shown in Fig 11.

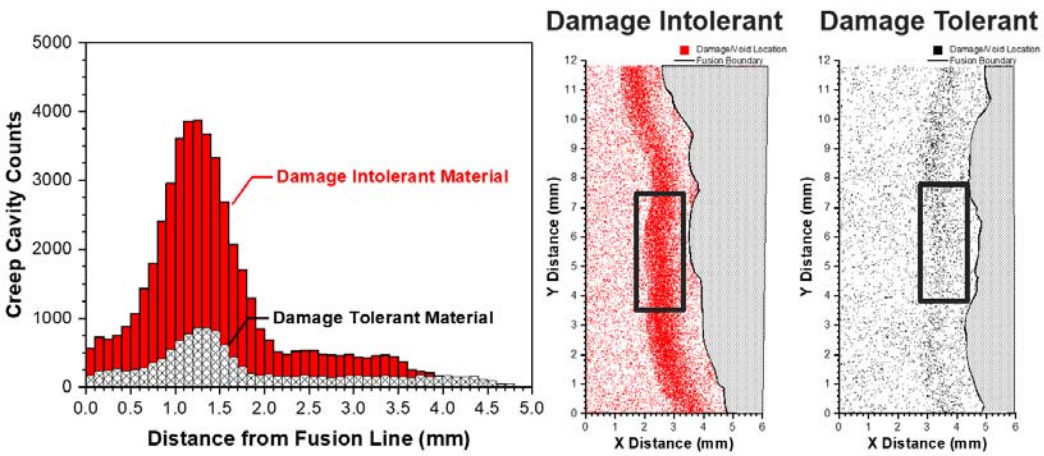

Figure 11: Comparison of creep cavity counts as a function of distance from the weld fusion boundary for damage tolerant sample DT-1 and damage intolerant sample DINT-4. NOTE: damage cavity maps show the total counts of damage and NOT size distribution.

Highlighted areas (shown as a black box outline) in the damage maps from Fig 11 were used to calculate the overall cavitation density in each heat of material. The damage intolerant material showed an average creep void density of ~ 2,900 voids/mm^2. The damage tolerant material showed an average creep void density of ~ 400 voids/mm^2. Although there was a much larger accumulation of voids in the damage intolerant material, there was not an obvious linear indication in the analyzed field of view. The damage tolerant material had a much lower density of voids. Additionally, there were linear indications (micro-cracks) at several locations in the damage tolerant material at the same life fraction.

CONCLUSION

In this study, two different heats of Grade 91 were evaluated using feature type cross-weld creep tests to evaluate the detectability of damage at known life fractions. The damage tolerant material showed a greater tendency to form micro-cracks and macro cracks at smaller time fractions than for the damage intolerant material. The manifestation and evolution of damage for the two heats were dramatically different. The quantification of damage showed a variability in the HAZ damage density that was >5X. These differences also emphasize the importance of material pedigree on the formation, evolution and detectability of damage in the Grade 91 HAZ. In this study, PAUT successfully identified damage in the HAZ manifested as local cracking (of ~ 1 mm in length) in the damage tolerant material at a life fraction of ~80%. However, the same procedure was not able to identify linear indications nor high fields of creep damage in the damage intolerant material in the sample at ~95% life. This research is a critical step in linking NDE, metallography, and the variability in damage formation and evolution in 9%Cr CSEF steel HAZ material.

REFERENCES

[1] M. Yaguchi, T. Matsumura, and K. Hoshino. “Evaluation of Long-term Creep Strength of Welded Joints of ASME Grades 91, 92 and 122 Type Steels.” Proceedings of the ASME 2012 Pressure Vessels and Piping Conference, Toronto, CA. PaperPVP2012-78393. pp. 317–326.

[2] N. Nishimura, M. Ozaki and F. Masuyama. “The Effect of the Tramp Elements on the Creep Property of the Modified 9Cr-1Mo Steel.” 5th International Conference on Clean Steel, Vol. 2, 1997. pp. 117–125.

[3] Parker, Jonathan, and John Siefert. “Metallurgical and Stress State Factors Which Affect the Creep and Fracture Behavior of 9% Cr Steels.” Advances in Materials Science and Engineering, vol. 2018, 2018, pp. 1–15., doi:10.1155/2018/6789563.

[4] Sawada, K., et al. “Microstructural Degradation of Gr.91 Steel during Creep under Low Stress.” Materials Science and Engineering: A, vol. 528, no. 16-17, 2011, pp. 5511–5518., 2011.03.073.

[5] Siefert, J.A., and J.D. Parker. “Evaluation of the Creep Cavitation Behavior in Grade 91 Steels.” International Journal of Pressure Vessels and Piping, vol. 138, 2016, pp. 31–44., 2016.02.018.

[6] Parker, Jonathan, and Steve Brett. “Creep Performance of a Grade 91 Header.” International Journal of Pressure Vessels and Piping, vol. 111-112, 2013, pp. 82–88., 2013.05.003.

[7] Life Management of 9%Cr Steels: Evaluation of Metallurgical Risk Factors in Grade 91 Steel Parent Material. EPRI, Palo Alto, CA: 2018. 3002009678.

[8] “SA-335/SA-335M Specification for Seamless Ferritic Alloy-Steel Pipe for High-Temperature Service.” ASME B&PV Code Section II, Part A, 2017 edition.

[9] A. Nitsche, D. Allen and P. Mayr. "Damage Assessment of Creep Affected Weldments of a Grade 91 Header Component after Long-term High Temperature Service." Welding in the World 59 (4), 2015. pp. 675 to 682.

[10] Creep Rupture and Creep-Fatigue Behavior of Grade 91 and 92 Steels. EPRI, Palo Alto, CA: 2018. 3002009679.

[11] Nondestructive Methods for Detection of High-Temperature Damage in Creep-Strength-Enhanced Ferritic Steels (Grades 91 and 92) as a Basis for Life Evaluation. EPRI, Palo Alto, CA: 2015. 3002005187

[12] J. A. Siefert, J. D. Parker and R. C. Thomson. “Linking the Cross-weld Creep Performance to the As-fabricated Condition in Grade 91 Steel: Macro-based Assessment.” Welding Journal 98 (3), 2019. pp. 63-s to 77-s.